https://doi.org/10.5194/egusphere-2026-4822
Preprint. Discussion started: 24 August 2026

Environmental controls on methanotrophic oxidation capacity in the southeastern North Sea

Yanan Zhao[1], Vera Sidorenko[1], Carsten Lemmen[2] and Ingeborg Bussmann[3]

[1]Alfred Wegener Institute, Helmholtz Centre for Polar and Marine Research, 27570 Bremerhaven, Germany
[2]Institute of Systems Analysis and Modeling, Helmholtz-Zentrum Hereon, 21502 Geesthacht, Germany
[3]Alfred Wegener Institute, Helmholtz Centre for Polar and Marine Research, 27498 Helgoland, Germany

Correspondence to: Yanan Zhao (yanan.zhao@awi.de)

Abstract. Shallow coastal seas contribute disproportionately to marine methane (CH_4) emissions, yet the efficiency of the microbial sink that attenuates them remains poorly constrained. Under first-order kinetics, aerobic methane oxidation (MOx) is the product of ambient CH_4 concentration and the fractional turnover rate k', the latter representing the oxidation capacity of the methanotrophic community. Here we test whether k' can be predicted from routinely measured environmental variables, drawing on water samples collected during repeated campaigns between 2010 and 2014 across riverine, estuarine, and marine waters of the Elbe and the adjacent southeastern North Sea. In the estuary and adjacent marine waters, a second-order polynomial model based on temperature, salinity, and nitrate reproduced 80 % of the observed spatiotemporal variability in k' under five-fold cross-validation, indicating that these predictors captured the main environmental controls on k' and that nonlinear interaction terms cannot be omitted. Neither ambient CH_4 concentration nor phosphate improved model performance, indicating that k' is not directly controlled by substrate availability or phosphorus limitation. In riverine waters, by contrast, the same approach systematically underpredicted k' with large uncertainty, suggesting a distinct regional response regime that is likely linked to river-specific environmental controls. Overall, our results highlight that k' can be parameterized as a dynamic, environmentally dependent term, opening a route to estimating MOx in coastal systems.

https://doi.org/10.5194/egusphere-2026-4822
Preprint. Discussion started: 24 August 2026

1 Introduction

Methane (CH_4) is a potent greenhouse gas whose atmospheric concentration has increased continuously since the industrial era, contributing about 16 % of post-industrial radiative forcing (Forster, P. et al., 2021). Although the ocean is a comparatively modest net source of atmospheric CH_4, with global emissions estimated at 6 to 12 Tg yr^{-1}, this flux is highly uneven in space, with shallow coastal and shelf environments contributing disproportionately despite occupying only a minor fraction of total ocean area (Weber et al., 2019). In these shallow coastal environments, methanogenic archaea in anoxic sediments produce substantial amounts of CH_4, which can be transferred to the overlying water column by molecular diffusion, porewater advection, and ebullition (Egger et al., 2018; Hermans et al., 2024). Before this dissolved CH_4 can escape to the atmosphere, however, it encounters a final biological sink in the water column: aerobic methane oxidation (MOx) primarily mediated by methanotrophic bacteria. The amount of CH_4 removed by MOx before atmospheric release remains poorly constrained in coastal carbon budgets, with a global estimate of 1.8 ± 2.7 Tg yr^{-1} (Mao et al., 2022).

A useful way to quantify microbial CH_4 removal is the fractional turnover rate, k' (d^{-1}; Table 1). Assuming first-order kinetics, the MOx rate (nmol L^{-1} d^{-1}) can be calculated by multiplying the dissolved CH_4 concentration by k'. Here, k' describes the fraction of the dissolved CH_4 pool oxidized per unit time. It therefore represents an integrated outcome of active methanotroph abundance, community composition, and cell specific metabolic activity. Field studies have shown that k' can vary by orders of magnitude across aquatic environments (Bussmann et al., 2017). However, the environmental and biological controls underlying this variability remain poorly constrained, particularly in coastal systems where biotic and abiotic conditions are highly dynamic.

https://doi.org/10.5194/egusphere-2026-4822
Preprint. Discussion started: 24 August 2026

47 The southeastern North Sea provides a natural laboratory in which to examine these controls.
48 The Elbe and Weser rivers deliver methane-enriched freshwater with concentrations one to two
49 orders of magnitude above atmospheric equilibrium, while the adjacent Wadden Sea tidal flats
50 export biogenic methane through tidal pumping, together sustaining pronounced CH_4 gradients
51 across the estuarine-coastal interface (Grunwald et al., 2009; Osudar et al., 2015). Although
52 methane oxidation has been relatively well constrained in this system, its contribution to the total
53 CH_4 loss budget varies strongly seasonally, accounting for about 5 % in winter/spring and about
54

55 **Table 1**. Overview of methane-related terms used in this study.

Term	Symbol	Unit	Definition in this study
Fractional turnover rate	k'	d^{-1}	First-order rate constant describing the fraction of the dissolved CH_4 pool oxidized per unit time.
Dissolved methane concentration	$[CH_4]$	nmol L^{-1}	Dissolved CH_4 concentration in the water column.
Aerobic methane oxidation	MOx	-	Microbial process of aerobic CH_4 oxidation under oxic conditions.
Methane oxidation rate	MOx rate	nmol L^{-1} d^{-1}	Rate of the MOx process; calculated as $k' \times [CH_4]$.

56

https://doi.org/10.5194/egusphere-2026-4822
Preprint. Discussion started: 24 August 2026

41 % in summer/fall (Matoušů et al., 2017). This pronounced seasonal contrast suggests that water-column CH_4 oxidation is highly dynamic and likely controlled by multiple interacting environmental factors. For instance, temperature can affect microbial metabolic rates and community composition (Mohanty et al., 2007; Sundh et al., 2005), while salinity gradients may constrain methane oxidation across river–sea transitions (Osudar et al., 2017a). Suspended particulate matter, oxygen availability, and nutrient supply may further influence methanotrophic activity by altering particle associated habitats, redox conditions, and growth constraints (Abril et al., 2007; Bodelier et al., 2000; Steinle et al., 2017). In addition, hydrodynamic processes can redistribute water masses and microbial communities, generating spatial heterogeneity in k' (Steinle et al., 2015; Wilkins et al., 2013). Together, these studies suggest that k' variability is shaped by the combined influence of physicochemical parameters, motivating a multivariate modelling approach to reconstruct k' from multiple environmental variables.

Despite its central role in methane oxidation, direct determination of k' remains methodologically demanding, typically relying on labor-intensive radiotracer-based incubations that yield sparse and temporally discontinuous observations (Bussmann et al., 2015). This practical limitation has constrained efforts to resolve the environmental controls on k' and to incorporate methanotrophic capacity explicitly into water-column methane budgets. To our knowledge, no previous study has directly modelled the spatiotemporal variability of k'. Here, we address this gap using observations from repeated field campaigns conducted in the southeastern North Sea between 2010 and 2014. The aims of this study are: i), to quantify the spatiotemporal variability of k' across a river-estuary-marine gradient; ii), to identify the major environmental factors associated with k'; and iii), to evaluate whether k' can be reconstructed from environmental

https://doi.org/10.5194/egusphere-2026-4822
Preprint. Discussion started: 24 August 2026

variables. These analyses are intended to support a more process-based representation of methanotrophic capacity in coastal methane budgets.

2 Methods

2.1 Study area and available observations

The study area encompasses the Elbe Estuary and the adjacent German Bight, a shallow coastal system with typical water depths generally below 50 m (Jacob and Stanev, 2021). The region is hydrographically dynamic, characterized by a large tidal range from 1.5 to 3.6 m (Fofonova et al., 2019; Gräwe et al., 2016; Plüß, Andreas, 2003). The German Bight is directly influenced by the discharge of three relatively large rivers, the Elbe, Weser, and Ems (Becker et al., 1992). The freshwater input leads to intermittent stratification, mediated by tidal and wind forcing in the estuaries and central German Bight. The relatively fresh coastal waters form a buoyancy-driven current along the coast, mediated by Earth's rotation. The transect from the inner estuary to the open German Bight therefore spans a natural gradient of riverine, estuarine, and marine conditions. Sampling stations were classified into three categories based on the median salinity of all samples collected at each station (Fig. 1): riverine water (salinity < 5, in PSU), estuarine water (5 ≤ salinity ≤ 30), and marine water (salinity > 30). These categories correspond to sampling stations located at 9.09° E–10.03° E, 8.41° E–8.80° E, and 7.89° E–8.31° E, respectively.

This study draws on a harmonized dataset compiled from repeated campaigns conducted between October 2010 and November 2014 (Hackbusch et al., 2019; Matoušů et al., 2017; Osudar et al., 2015), with a specific focus on the fractional turnover rate k'. At each station, discrete water samples were collected using Niskin bottles from two depth layers: the surface layer (approximately 1 m below the surface) and near bottom waters (approximately 1 m above the

https://doi.org/10.5194/egusphere-2026-4822
Preprint. Discussion started: 24 August 2026

sediment). Measured parameters included CH_4 concentration and k', together with temperature, salinity, dissolved oxygen, inorganic nutrients (NO_2^-, NO_3^-, NH_4^+, PO_4^{3-} and silicate), SPM and water depth (Table 2). Analytical procedures are summarized in Supplementary Text S1. The observational datasets used in this study are archived in PANGAEA (Bussmann et al., 2014b, a, 2019; Matousu et al., 2015).

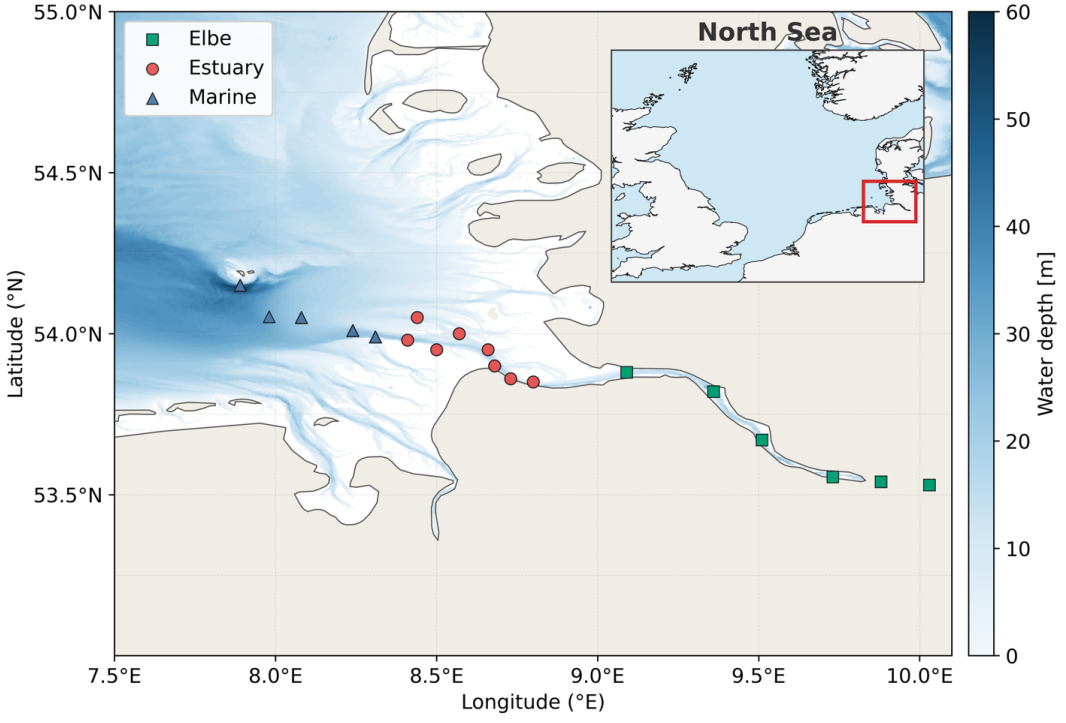

Figure 1. Map of the southeastern North Sea showing the locations of sampling stations, classified into three categories according to the median salinity of all samples collected at each station: the Elbe (median salinity < 5, green squares), the estuary (5 ≤ median salinity ≤ 30, red circles), and the marine region (median salinity > 30, blue triangles). Background shading indicates water depth (m).

https://doi.org/10.5194/egusphere-2026-4822
Preprint. Discussion started: 24 August 2026

2.2 Statistical analysis

Spearman's rank correlation coefficient (r_s) was used to assess pairwise relationships between variables, with statistical significance set at $p < 0.01$. Differences between paired surface and bottom samples were tested using the Wilcoxon signed-rank test, as the paired differences did not meet the Shapiro-Wilk normality assumption required for a paired t-test.

2.3 Polynomial regression

Polynomial regression models were used to evaluate whether k' could be estimated from routinely measured environmental variables. A simple linear model may be too restrictive because it assumes additive effects with constant slopes across the full environmental range and does not account for interactions among predictors. As a subset of GAMs, polynomial regression therefore provides a simple parametric framework for testing whether curvature and pairwise interactions improve the reconstruction of k' while retaining interpretability (James et al., 2021).

Models were fitted to k' using 11 candidate predictors: CH_4 concentration, temperature, salinity, dissolved oxygen, SPM, water depth, and dissolved nutrients (NO_2^-, NO_3^-, NH_4^+, PO_4^{3-}, and silicate). Polynomial degrees of 1–3 were evaluated across all predictor combinations containing up to five base predictors, thereby limiting model complexity and reducing overfitting (e.g., Fig. 4). Model performance was assessed using repeated five-fold cross-validation with 100 repeats. Within each split, predictors were standardized using parameters estimated from the training folds and then applied to the validation fold. Out-of-fold predictions were used to calculate the coefficient of determination (R^2), root mean squared error (RMSE), and mean absolute error (MAE), and metrics were summarized across repeats. Variance inflation factors (VIFs) were calculated for the base predictors to assess multicollinearity (Table S1). Exploratory analyses were initially performed using all samples. Because the Elbe samples showed response patterns distinct

https://doi.org/10.5194/egusphere-2026-4822
Preprint. Discussion started: 24 August 2026

from those of the marine-estuary samples (Fig. S1), models were subsequently built separately for the marine-estuary and river regions.

3 Results

3.1 Environmental setting

Environmental variability in the southeastern North Sea was characterized by a strong seasonal temperature cycle, a pronounced river-to-marine salinity gradient, and nutrient enrichment associated with the Elbe River (Table 2). Based on the station-median salinity classification described above, the dataset covered three hydrographic regions: the Elbe, estuarine, and marine regions. Water temperature ranged from 1.4 to 22.2 °C and was driven primarily by season, whereas longitudinal variation in temperature was comparatively weak. In contrast, salinity increased strongly from the freshwater Elbe region toward the marine stations, spanning 0–33.6 PSU across the full dataset, with the largest variability occurring in the estuarine mixing zone.

Nitrate spanned nearly four orders of magnitude, from 0.3 to 1659 µmol L^{-1}, and generally decreased from the Elbe region through the estuary to the marine region. Phosphate, nitrite, ammonium and silicate broadly followed the same decreasing gradient, consistent with a dominant riverine source. Dissolved oxygen concentrations were above the hypoxic threshold of 2 mg L^{-1} throughout the study period, with a minimum concentration of 3.6 mg L^{-1}. Suspended particulate matter (SPM) ranged from 6 to 832 mg L^{-1}, with a pronounced peak at 9.36° E (station median 160 mg L^{-1}), coinciding with the Elbe estuarine turbidity maximum reported by (Kappenberg and Grabemann, 2001). Vertical gradients were generally weak during all campaigns. Temperature and most nutrients showed no consistent surface to bottom differences, whereas SPM was elevated near the bottom, due to bottom shear stress.

https://doi.org/10.5194/egusphere-2026-4822
Preprint. Discussion started: 24 August 2026

Table 2. Overview of physicochemical parameters in the water column during all sampling campaigns from October 2010 to November 2014. Median ± standard deviation and the range of the data (in brackets) are given. Sampling stations were grouped into three hydrographic regions: marine stations with median salinity > 30 PSU (7.89–8.31° E), estuarine stations with median salinity 5–30 PSU (8.41–8.80° E), and Elbe stations with median salinity < 5 PSU (9.09–10.03° E).

Station [° E]	Salinity [PSU]	Temperature [°C]	Oxygen [mg L^{-1}]	SiO4 [µmol L^{-1}]	PO4 [µmol L^{-1}]	NO2 [µmol L^{-1}]	NO3 [µmol L^{-1}]	NH4 [µmol L^{-1}]	SPM [mg L^{-1}]
Marine stations									
7.89	32.5 ± 0.9 [30.2–33.6]	9.8 ± 5.2 [4.2–18.5]	8.6 ± 1.3 [6.1–10.6]	6.0 ± 5.3 [0.5–18.9]	0.5 ± 1.3 [0.1–5.4]	0.4 ± 1.9 [0–6.1]	3.2 ± 8.2 [0.4–28.2]	1.3 ± 0.9 [0–3.9]	74 ± 18 [43–104]
7.99	31.6 ± 1.3 [28.5–33.5]	9.3 ± 5.5 [3.8–18.2]	9.4 ± 1.5 [6.0–11.3]	8.0 ± 8.2 [2.6–31.5]	0.8 ± 0.4 [0.1–1.6]	0.4 ± 0.4 [0–1.1]	5.4 ± 11.6 [0.3–42.1]	2.1 ± 0.7 [0.6–3.1]	71 ± 33 [15–149]
8.08	31.6 ± 2.0 [27.0–32.6]	6.3 ± 1.7 [2.8–6.8]	10.1 ± 0.9 [9.1–11.5]	17.4 ± 12.2 [6.6–40.9]	0.8 ± 0.2 [0.7–1.2]	0.8 ± 0.2 [0.7–1.2]	20.4 ± 17.4 [6.5–54.9]	3.0 ± 0.7 [2.5–4.4]	86 ± 17 [59–111]
8.24	31.4 ± 0.9 [29.6–33.1]	11.0 ± 5.4 [2.8–18.9]	8.5 ± 1.2 [7.3–11.3]	10.1 ± 9.1 [1.3–28.8]	0.8 ± 0.4 [0.3–1.7]	0.6 ± 0.4 [0.2–1.4]	7.5 ± 12.4 [0.5–37.7]	2.5 ± 1.5 [0.2–5.2]	87 ± 29 [8–134]
8.31	30.7 ± 1.4 [27.1–33.0]	8.4 ± 5.9 [2.1–19.3]	8.4 ± 1.4 [6.2–11.6]	14.0 ± 12.1 [0.8–42.5]	0.8 ± 0.5 [0.1–2.0]	0.6 ± 0.4 [0.2–1.4]	13.7 ± 14.6 [0.6–44.5]	2.2 ± 1.6 [0.1–5.9]	91 ± 25 [18–132]
Estuarine stations									
8.41	29.8 ± 2.1 [23.5–32.8]	11.0 ± 6.1 [2.1–19.9]	9.5 ± 1.2 [7.5–11.4]	13.0 ± 16.5 [0–68.1]	0.9 ± 0.5 [0.4–2.2]	0.7 ± 0.5 [0.2–1.7]	19.3 ± 31.7 [1.2–131]	3.0 ± 1.5 [0.2–6.0]	91 ± 31 [15–136]
8.44	28.3 ± 2.0 [24.1–31.8]	9.0 ± 5.1 [2.6–18.1]	10.5 ± 3.1 [5.2–13.3]	22.2 ± 25.6 [1.6–80.8]	1.3 ± 0.9 [0.1–3.2]	0.9 ± 0.8 [0.2–2.6]	47.1 ± 382 [17.5–1037]	6.6 ± 4.5 [3.8–16.5]	104 ± 35 [28–157]
8.50	26.6 ± 3.0 [19.4–32.1]	7.7 ± 6.5 [1.7–20.3]	9.7 ± 1.2 [8.0–11.9]	18.8 ± 27.0 [0.8–92.1]	1.2 ± 0.5 [0.4–1.9]	1.0 ± 0.6 [0.2–1.9]	47.4 ± 34.8 [6.0–130]	3.6 ± 1.8 [0.7–8.1]	93 ± 25 [72–167]

https://doi.org/10.5194/egusphere-2026-4822
Preprint. Discussion started: 24 August 2026

8.57	24.6 ± 46.0 [9.6–28.2]	9.0 ± 5.3 [2.7–17.7]	8.6 ± 2.2 [5.3–11.3]	32.9 ± 19.5 [1.7–65.2]	1.7 ± 0.7 [0.2–2.4]	0.8 ± 0.7 [0.3–2.6]	49.1 ± 224 [18.3–856]	7.4 ± 4.0 [3.4–15.7]	99 ± 30 [30–157]
8.66	22.9 ± 6.4 [6.0–26.3]	10.1 ± 5.5 [1.8–18.0]	8.8 ± 1.7 [7.6–12.5]	30.4 ± 20.4 [3.9–63.6]	1.4 ± 0.6 [0.4–3.0]	1.0 ± 0.7 [0.3–2.6]	81.8 ± 78.0 [35.3–264]	6.4 ± 3.8 [2.9–13.4]	101 ± 28 [31–147]
8.68	19.2 ± 4.6 [9.9–27.7]	6.8 ± 6.8 [1.4–21.1]	9.2 ± 1.7 [7.9–12.9]	45.5 ± 50.6 [0–156]	1.8 ± 0.8 [0.3–3.3]	1.1 ± 0.7 [0.1–2.4]	53.4 ± 49.3 [14.0–219]	5.2 ± 3.6 [0.8–14.6]	89 ± 22 [59–152]
8.73	15.1 ± 5.6 [0.3–23.2]	10.6 ± 5.0 [4.2–20.1]	8.4 ± 1.7 [5.3–11.0]	62.7 ± 30.8 [14.5–109]	1.9 ± 0.6 [1.1–3.2]	1.0 ± 0.7 [0.5–2.6]	129 ± 477 [60.0–1659]	6.9 ± 2.7 [2.7–12.4]	99 ± 51 [45–216]
8.80	12.1 ± 5.1 [0.2–17.8]	11.2 ± 5.1 [4.1–20.5]	8.2 ± 1.7 [5.5–11.1]	75.7 ± 43.8 [17.1–169]	2.2 ± 2.5 [1.4–14.1]	1.0 ± 0.7 [0.2–2.6]	173 ± 441 [40.0–1659]	5.4 ± 2.7 [2.2–11.3]	90 ± 53 [56–332]
Riverine stations									
9.09	3.2 ± 3.0 [0.1–13.7]	12.1 ± 5.3 [3.9–21.5]	8.2 ± 1.8 [5.5–12.0]	99.4 ± 50.6 [20.8–185]	2.5 ± 2.3 [1.2–11.9]	0.5 ± 0.7 [0–2.6]	207 ± 440 [75.7–1619]	4.0 ± 2.6 [0.9–9.5]	96 ± 119 [29–502]
9.36	0.7 ± 0.6 [0–3.0]	13.3 ± 5.7 [3.4–21.0]	8.0 ± 1.9 [5.3–11.7]	129 ± 48.1 [12.0–170]	1.6 ± 1.9 [0.9–8.4]	0.3 ± 0.8 [0–2.7]	226 ± 395 [116–1510]	3.0 ± 3.4 [0.5–15.7]	160 ± 130 [31–525]
9.51	0.5 ± 0.2 [0–0.9]	10.8 ± 5.6 [4.4–20.9]	8.1 ± 2.1 [5.1–11.5]	110 ± 50.2 [1.7–173]	1.4 ± 1.5 [0.6–6.5]	1.0 ± 0.9 [0–2.5]	251 ± 422 [81–1524]	3.0 ± 3.4 [1.5–15.1]	76 ± 72 [14–258]
9.73	0.3 ± 0.2 [0–0.7]	13.6 ± 5.8 [4.4–21.8]	8.9 ± 2.3 [4.9–11.9]	131 ± 52.9 [0–213]	1.4 ± 1.5 [1.0–6.2]	1.7 ± 0.9 [0–4.1]	260 ± 396 [65–1490]	5.0 ± 3.5 [1.9–12.9]	32 ± 159 [12–832]
9.88	0.4 ± 0.2 [0–0.6]	10.5 ± 5.1 [5.1–22.2]	8.5 ± 2.7 [3.6–11.2]	134 ± 49.8 [0–171.7]	1.3 ± 0.9 [0.4–3.7]	1.4 ± 1.0 [0.7–4.3]	236± 410 [119–1387]	6.4 ± 3.0 [3.1–12.6]	20 ± 29 [6–120]
10.03	0.4 ± 0.2 [0–0.7]	13.6 ± 5.4 [5.2–21.9]	8.2 ± 1.6 [6.4–10.9]	138 ± 54.8 [0–179]	1.4 ± 1.5 [0.1–4.8]	1.4 ± 0.8 [0.6–3.8]	262 ± 405 [128–1451]	6.4 ± 5.2 [3.6–20.4]	21 ± 12 [8–52]

166

https://doi.org/10.5194/egusphere-2026-4822
Preprint. Discussion started: 24 August 2026

3.2 The fractional turnover rate *k'*, and correlations analysis with abiotic conditions

The fractional turnover rate k' increased from the marine region toward the river, with regional medians of 0.02 d^{-1} in the marine region, 0.04 d^{-1} in the estuary and 0.43 d^{-1} in the Elbe with maxima reaching 2.86 d^{-1} (Fig. 2a). The higher and more variable k' values in the riverine region may be partly explained by the elevated methanotroph abundance previously reported for the Elbe (Hackbusch et al., 2019). Dissolved CH_4 concentrations also showed a pronounced gradient, ranging from 5 to 2306 nmol L^{-1} (Fig. 2b). Concentrations were lowest in the marine region, with a regional median of 15 nmol L^{-1}, increased in the estuary to 43 nmol L^{-1}, and reached the highest concentrations in the river, where the median concentration was 66 nmol L^{-1} and maximum values exceeded 2300 nmol L^{-1}. MOx ranged from 0.01 to 5542.3 nmol L^{-1} d^{-1} and followed the same marine-river gradient. Regional median MOx values increased from 0.20 nmol L^{-1} d^{-1} in the marine region to 1.88 nmol L^{-1} d^{-1} in the estuarine region and 32.25 nmol L^{-1} d^{-1} in the Elbe region (Fig. 2b). Across regions, k' and CH_4 showed similar spatial gradients, but their weak correlation indicates that they were partly decoupled (Fig. 3); also, no logarithmic relationship as expected from Michaelis–Menten kinetic was observed.

Correlations between k' and environmental variables were region dependent and generally insufficient to explain variability in k' (Fig. 3). Marine waters are characterized by relatively low variation in k' which shows no clear correlation with environmental factors that vary only slightly (Fig. 3a). In contrast, the estuarine zone showed clearer environmental structure: k' was negatively associated with salinity ($r_s = -0.58$) and positively associated with temperature ($r_s = 0.61$), indicating that both the estuarine mixing gradient and seasonal temperature conditions were linked to methanotrophic oxidation capacity. In the Elbe region, k' was moderately correlated with

https://doi.org/10.5194/egusphere-2026-4822
Preprint. Discussion started: 24 August 2026

temperature (r_s = 0.49), but no other environmental variable showed a clear relationship with k', suggesting a more complex freshwater process regime.

No significant surface-bottom differences in k', CH_4 concentration or MOx rates were detected across regions; therefore, surface and bottom samples were pooled. Overall, the correlation analysis provided a first overview of region-specific monotonic relationships, but it could not account for nonlinear or combined effects among predictors. The next section therefore evaluates whether nonlinear multivariate models can better predict k' across the regions.

https://doi.org/10.5194/egusphere-2026-4822
Preprint. Discussion started: 24 August 2026

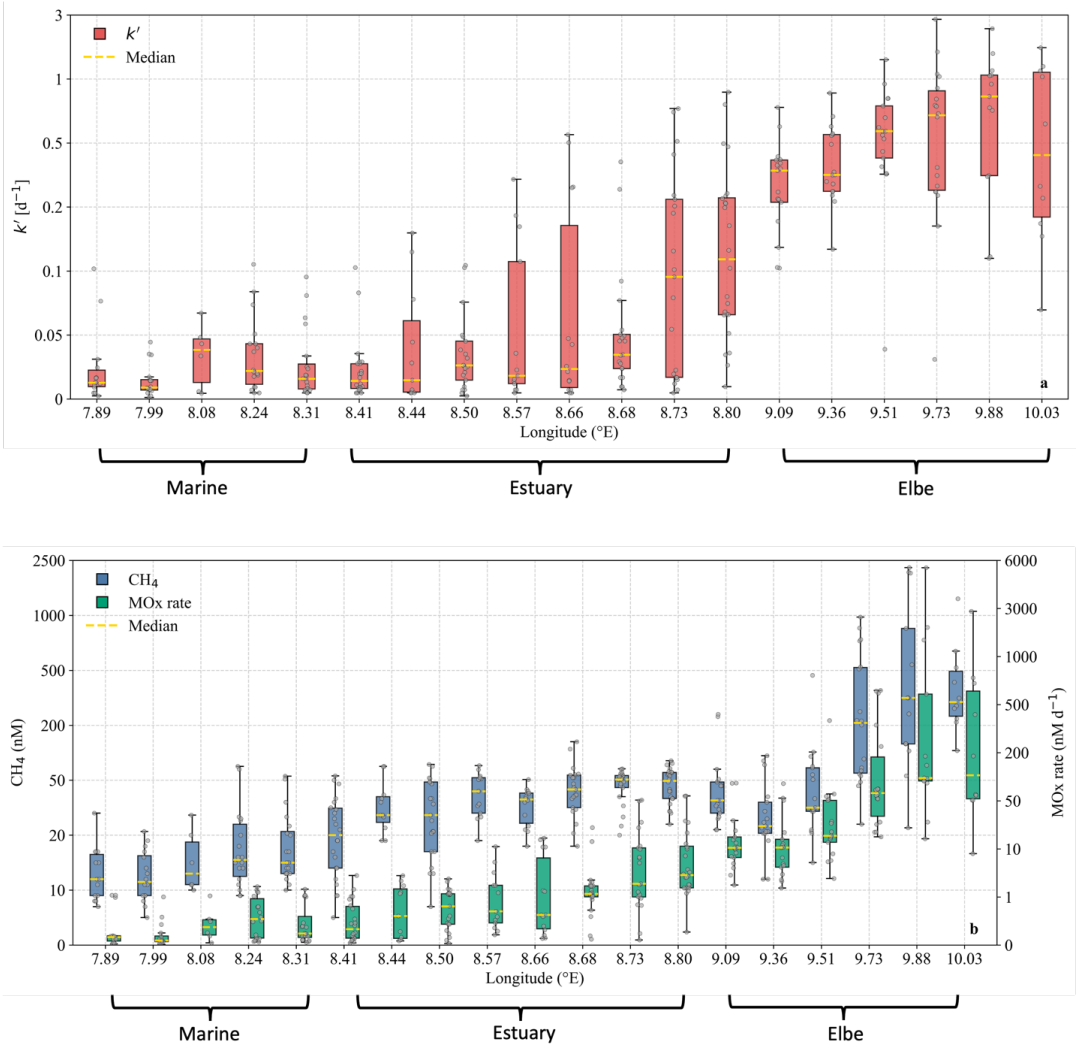

Figure 2. Longitudinal distributions of the fractional turnover rate *k*′, dissolved CH_4 concentration and MOx rate across the marine, estuarine and Elbe regions. (a) Fractional turnover rate *k'*. (b) Dissolved CH_4 concentration and MOx rate. Boxplots show the median and interquartile range at each station, and grey dots represent observations. Please note that all y-axes are displayed on non-linear scales for visualization.

https://doi.org/10.5194/egusphere-2026-4822
Preprint. Discussion started: 24 August 2026

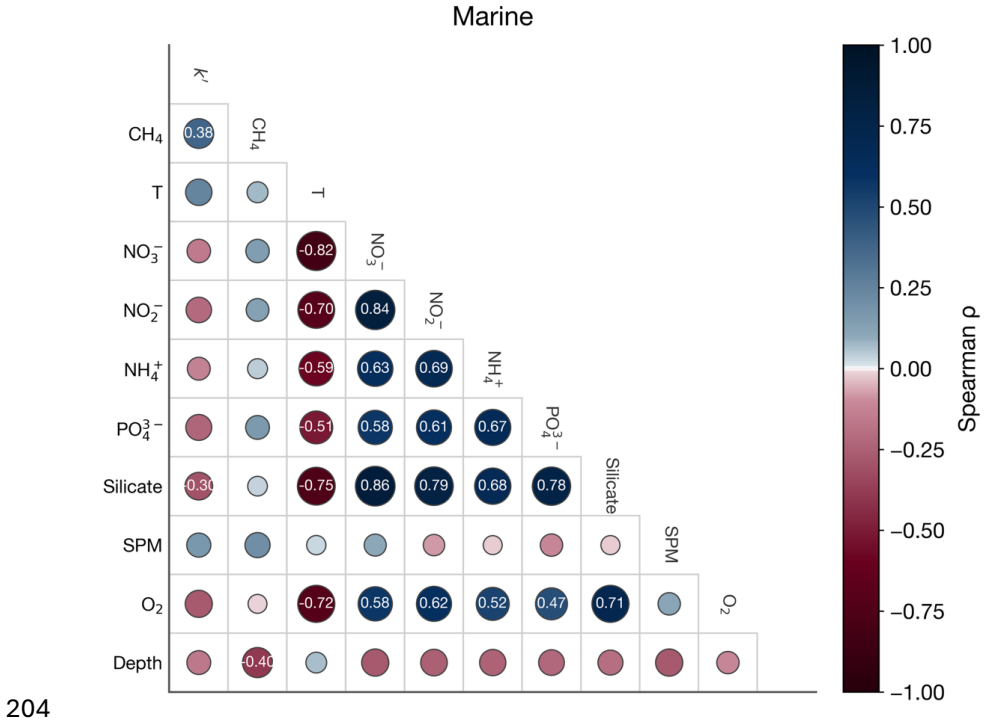

204

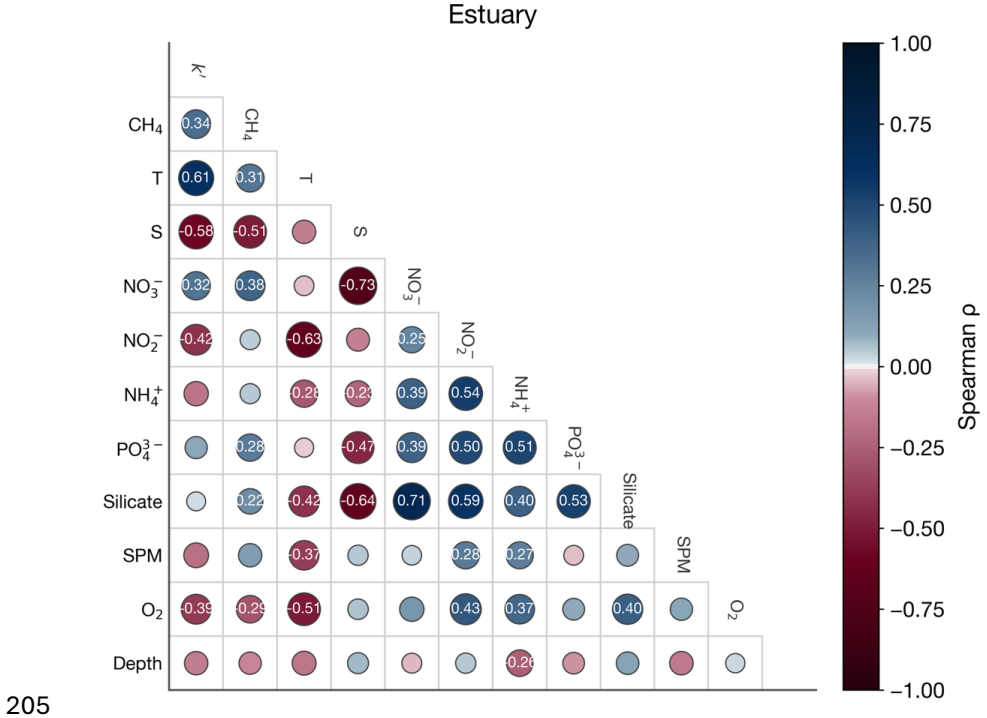

205

https://doi.org/10.5194/egusphere-2026-4822
Preprint. Discussion started: 24 August 2026

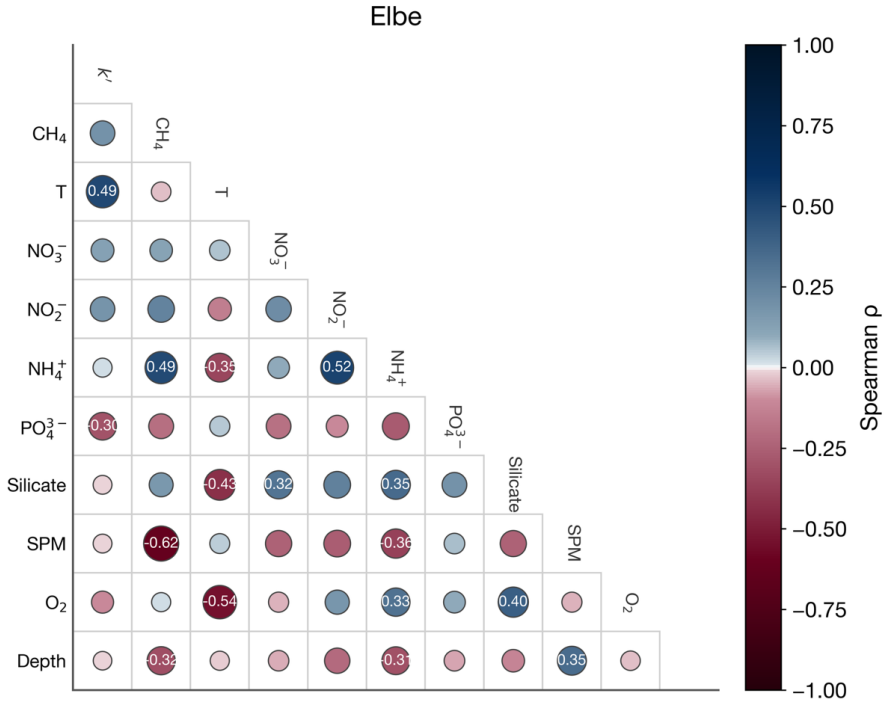

Figure 3. Spearman rank correlation coefficients between the fractional turnover rate (k'), CH_4 concentration and environmental parameters across the three hydrographic regions (marine, estuary, and Elbe). Numbers are shown only for correlations significant at the $p < 0.01$ level (two-tailed). T stands for temperature and S stands for salinity. Salinity was excluded from the coastal marine and Elbe matrices because it showed little variability within these regions.

https://doi.org/10.5194/egusphere-2026-4822
Preprint. Discussion started: 24 August 2026

3.3 Non-linear approach on the fractional turnover rate (*k'*)

In the marine-estuarine regions, the second-degree polynomial model using temperature, salinity, and NO_3^- as base predictors provided the best predictive performance relative to model complexity. Lower-degree models underfit the data, whereas higher-degree models showed signs of overfitting (Fig. 4a). Adding further variables to the selected T + S + NO_3^- framework, including CH_4 concentration, O_2, SPM, and water depth, did not improve cross-validated prediction sufficiently to justify their inclusion in the model. The squared NO_3^- term was removed from the expansion because its coefficient showed large variability across validation repeats, and its exclusion did not reduce repeated cross-validation performance (Table S1). VIF values for the base predictors were all below 2, indicating that multicollinearity among temperature, salinity, and NO_3^- was low and unlikely to affect model stability. The model (T + S + NO_3^-, polynomial degree = 2) reproduced the major variability in k' across the estuarine and marine regions (Fig. 4). Model performance was comparable between training and validation subsets, with $R^2 = 0.85 \pm 0.03$, RMSE = 0.06 d^{-1}, and MAE = 0.04 d^{-1} for training, and $R^2 = 0.82 \pm 0.01$, RMSE = 0.06 d^{-1}, and MAE = 0.04 d^{-1} for validation. The mean residual (observation - prediction) was close to zero, indicating little overall bias.

As noted above, when all samples were included in model training, k' in the Elbe samples exhibited patterns distinct from those from the marine-estuary regions. Residuals in the Elbe were predominantly positive, indicating systematic underprediction of riverine k' (Fig. S1). Accordingly, Elbe-specific models were developed using the same model selection framework as for the marine-estuarine models. Candidate models were also constructed from the 11 available environmental variables, with polynomial degrees ranging from 1 to 3 and with up to five predictors included in each model (Fig. 4b). However, their ability to reconstruct k' remained limited, as indicated by

https://doi.org/10.5194/egusphere-2026-4822
Preprint. Discussion started: 24 August 2026

lower R^2 values and higher uncertainty. This result was not confined to particular sampling seasons or stations, fresher-water samples (e.g., salinity < 0.5), or only to the highest k' observations (e.g., $k' > 1.0$ d^{-1}). Together, these findings suggest that riverine k' is governed by a distinct response regime that was not sufficiently captured by the predictors available in this study.

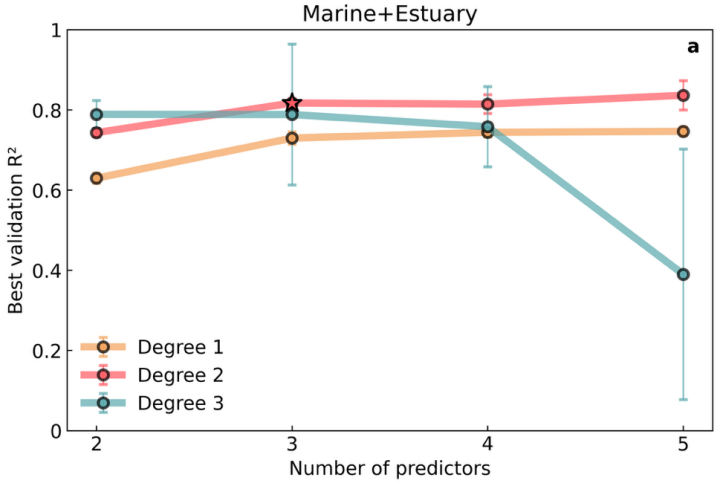

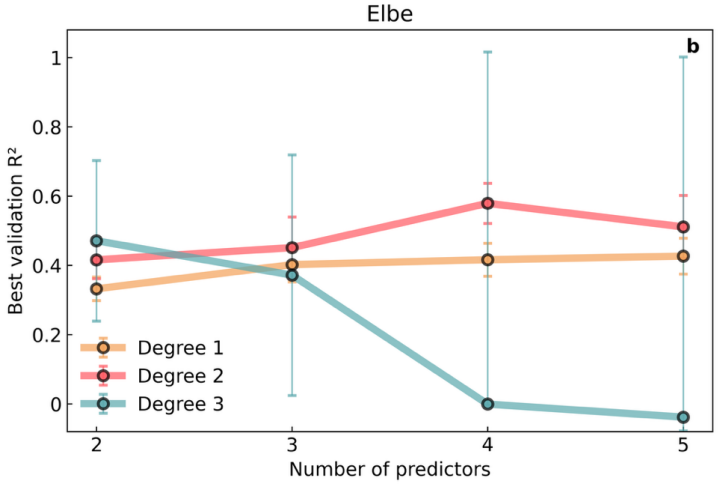

https://doi.org/10.5194/egusphere-2026-4822
Preprint. Discussion started: 24 August 2026

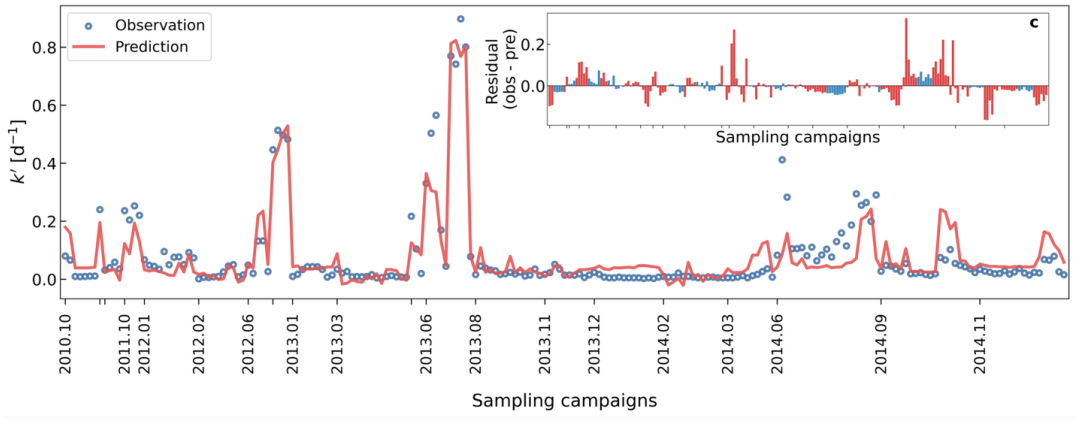

Figure 4. Model selection of k' using polynomial regression. Upper panels (a, b): Best repeated 5-fold cross-validation R^2 for each combination of polynomial degree (1–3) and number of predictors (2–5) in the Marine-Estuary (n = 203) and Elbe (n = 80) regions. Points indicate the highest mean validation R^2 among tested predictor combinations, and error bars show the standard deviation across repeated cross-validation estimates. The star marks the model selected for this study (T + S + NO_3^-); the Elbe panel uses a nonlinear y-axis for visualization. Lower panel (c): Reconstruction of k' in the marine-estuarine region from 2010 to 2014 (n = 203). Blue circles show observations, and the red line shows cross-validated predictions. The inset shows residuals calculated as observed minus predicted k'. Model performance metrics are reported as the mean ± standard deviation across repeated cross-validation runs. For readability, four selected campaign labels were omitted: 2010.11, 2010.12, 2012.08, and 2013.04.

https://doi.org/10.5194/egusphere-2026-4822
Preprint. Discussion started: 24 August 2026

4 Discussion

4.1 Environmental drivers of methanotrophic oxidation capacity

In our study, CH_4 concentration provided little explanatory information and showed only weak correlations with k'. From a microbiological point of view, k' should be related to CH_4 concentration according to the enzymatic relationship between maximal reaction rate and the substrate concentration (i.e. Michaelis–Menten kinetic). However, this decoupled relationship has been shown in previous studies that an increase in the methanotrophic oxidation capacity can be related to higher methanotroph abundance, higher cell-specific activity, or a shift toward different methanotroph groups, rather than through elevated CH_4 concentration alone (Baily et al., 2026; Mayr et al., 2020). In contrast to substrate availability, our study demonstrates k' variability was shaped by environmental variables, namely temperature, salinity, and NO_3^-, roles of these variables are discussed below.

At a broader scale, temperature and salinity can be interpreted as proxies for seasonality and water-mass mixing, respectively. Changes in these gradients may drive shifts and succession in methanotrophic community composition, thereby influencing k' (Deng et al., 2017; Harpenslager et al., 2026; Tobias-Hünefeldt et al., 2026). Beyond these indirect ecological effects, temperature and salinity may also directly affect the physiological state and activity of methanotrophs through changes in growth, cell-specific activity, thermal acclimation, and osmotic stress, although these effects are not independent (Lofton et al., 2014; Osudar et al., 2017b; Tveit et al., 2023). Consistent with these mechanisms, the polynomial model indicated a generally positive but nonlinear and interaction-dependent role of temperature, with positive T and T × NO_3^- terms but negative T^2 and T × S terms. In contrast, salinity-related terms were predominantly negative, including S, T × S,

https://doi.org/10.5194/egusphere-2026-4822
Preprint. Discussion started: 24 August 2026

and S × NO_3^-, while the positive S^2 term indicates that this association was not strictly linear (Table S1).

Adding NO_3^- to the T + S model improved model performance (e.g., Fig. 4a), suggesting that nitrate carried additional information. Biological uptake, organic matter remineralization, nitrification, and riverine nitrogen inputs can modify nitrate concentrations independently of salinity-driven mixing, particularly in the Elbe estuary, where internal nitrogen transformations strongly affect dissolved inorganic nitrogen dynamics (Dähnke et al., 2022; Sanders et al., 2018). In the polynomial model, the nitrate signal was expressed mainly through the T × NO_3^- interaction, suggesting that nitrate effects were linked to the temperature context. This interaction may reflect warm and nitrate-rich conditions that support higher active methanotroph biomass or activity. The biological interpretation is mechanistically plausible, as mineral nitrogen availability can support methanotroph growth and methane oxidation when nitrogen is limiting, although responses vary among systems and nitrogen forms (Bodelier et al., 2000; Bodelier and Laanbroek, 2004).

Other nutrient variables showed limited predictive performance. Although PO_4^{3-} is essential for microbial growth and can affect methanotroph physiology under phosphorus limitation (Nijman et al., 2022; Scanlan et al., 2022), PO_4^{3-} did not sufficiently improve validation in this dataset, suggesting that PO_4^{3-} availability was unlikely to be the dominant limiting factor for k'. Similarly, NO_2^- was not retained as a robust predictor, likely because it is a short-lived intermediate in nitrogen cycling and may inhibit methane oxidation at elevated concentrations, rather than serving as a stable indicator of methanotroph nutrient demand (Nyerges et al., 2010).

4.2 Unaccounted controls on k' in the Elbe

Methanotrophs show habitat specificity, and their occurrence and activity are shaped by multiple abiotic factors, including variables (e.g., pH and trace metals) not fully represented in our

https://doi.org/10.5194/egusphere-2026-4822
Preprint. Discussion started: 24 August 2026

dataset (Knief, 2015). In the Elbe and its downstream waters, these environmental gradients may create distinct microbial habitats, supporting spatial variability in methanotroph assemblages (Russnak et al., 2026), even among nearby sampling stations (Kaupper et al., 2022). Sediment-associated methanotrophs may add another source of variability, as differences in sedimentary conditions between upstream and downstream reaches may select for distinct assemblages that can enter the water column through resuspension or sediment-water exchange (Sherry et al., 2016; Tobias-Hünefeldt et al., 2026). Finally, hydrological and microbial legacy effects may weaken the relationship between k' and instantaneous predictors, because water-mass history, including travel time, downstream dispersal, and the time required for growth and succession, can shape microbial community structure and activity rather than abiotic conditions at the time of sampling alone (Bambakidis et al., 2024; Demeter et al., 2025).

The possibility that the range of predictors in the Elbe contributed to reduced model performance cannot be excluded. For example, salinity generally spanned a narrow freshwater range, reducing its ability as a proxy for water mass mixing. NO_3^- concentrations in the Elbe were generally higher compared to downstream waters, which likely reduced their sensitivity as a proxy for nutrient limitation or biogeochemical state. Oxygen is mechanistically central to aerobic methane oxidation. however, dissolved oxygen in our study remained within a narrow oxic range, so it was unlikely to be a limiting factor and consequently contributed little explanatory information to the model. This does not imply that oxygen is unimportant for methane oxidation; rather, it indicates that our measured gradient was probably too small to resolve oxygen-related controls on k' (Oswald et al., 2016).

4.3 Advantages and limitations of polynomial approach

https://doi.org/10.5194/egusphere-2026-4822
Preprint. Discussion started: 24 August 2026

The main advantage of the polynomial approach is its transparency and simple implementation. It provides an explicit approximation of k' as a function of environmental predictors, making the model feasible to interpret and to incorporate into numerical ocean models with an integrated methane module. Our study shows that the second-order polynomials provide a suitable approximation, and the inclusion of nonlinear terms improved model performance, whereas higher-degree polynomials showed signs of overfitting and would likely require larger datasets.

A key limitation is that the resulting approximation is likely region-specific. Temperature and salinity may be more broadly transferable predictors, as they reflect seasonal variability, mixing gradient, and potential shifts in microbial communities. In contrast, the roles of nutrients (e.g., nitrogen and phosphorus), dissolved oxygen, and other variables likely depend on the local hydrology, biogeochemical status, and methanotroph ecology. Therefore, the present model should be regarded as a transferable framework for developing region-specific polynomial parameterizations.

5 Conclusions

In this study, we examined whether the fractional turnover rate k' can be reconstructed from abiotic observations. In the estuarine and marine waters of the southeastern North Sea, a second-order polynomial in temperature, salinity, and nitrate reproduced most of the observed variability in k'. Ambient CH_4 concentration contributed no predictive information, suggesting that oxidation capacity is determined by the environmental conditions experienced by the methanotrophic community rather than by substrate supply. In the riverine Elbe, where k' was highest and most variable, none of the available abiotic predictors explained its variation, indicating additional controls beyond the abiotic variables considered here.

https://doi.org/10.5194/egusphere-2026-4822
Preprint. Discussion started: 24 August 2026

The model structure and selection procedure presented in this study are expected to apply to other coastal regions, whereas the fitted coefficients are region-specific and require refitting with local observations. Because k' responds to temperature and nutrient conditions, such parameterizations also allow the represented methane sink to adjust to ongoing coastal warming and changing nutrient loads, in contrast to representations based on fixed rate constants. Future work should incorporate microbial information, such as methanotroph abundance, community composition, and functional gene expression, to identify the biological controls underlying k' variability and to improve the representation of methane oxidation as a responsive biological sink in coastal methane cycling models.

Data availability

Data associated with this study are archived in the PANGAEA database under https://doi.org/10.1594/PANGAEA.833923, https://doi.org/10.1594/PANGAEA.833798, https://doi.org/10.1594/PANGAEA.855825, https://doi.org/10.1594/PANGAEA.897351.

Author contribution

Yanan Zhao: Conceptualization, Data curation, Formal analysis, Methodology, Visualization, Writing – original draft preparation. Vera Sidorenko: Conceptualization, Formal analysis, Methodology, Writing – review and editing. Carsten Lemmen: Formal analysis, Writing – review and editing. Ingeborg Bussmann: Investigation, Project administration, Supervision, Writing – review and editing.

Competing interests

https://doi.org/10.5194/egusphere-2026-4822
Preprint. Discussion started: 24 August 2026

Some authors are members of the editorial board of the journal. The authors have no other competing interests to declare.

Acknowledgements

ChatGPT (OpenAI) was used to improve clarity and readability of the manuscript.

Financial support

This study was funded by the Helmholtz Initiative InnoPool through the AGRIO project. This study is part of the Helmholtz program Changing Earth, subtopic 4.1: Fluxes and transformation of energy and matter in and across compartments.

https://doi.org/10.5194/egusphere-2026-4822
Preprint. Discussion started: 24 August 2026

388 References

389 Abril, G., Commarieu, M.-V., and Guérin, F.: Enhanced methane oxidation in an estuarine turbidity
390 maximum, Limnology & Oceanography, 52, 470–475, https://doi.org/10.4319/lo.2007.52.1.0470,
391 2007.

392 Baily, J. A., Hudspeth, Z. W., Morningstar, J. L., Mendlovitz, H. P., Martens, C. S., and Lloyd, K.
393 G.: Linking microbes to in situ methane oxidation rates in a eutrophic freshwater lake, Front.
394 Microbiol., 17, 1789101, https://doi.org/10.3389/fmicb.2026.1789101, 2026.

395 Bambakidis, T., Crump, B. C., Yoon, B., Kyzivat, E. D., Aho, K. S., Leal, C. F., Fair, J. H., Stubbins,
396 A., Wagner, S., Raymond, P. A., and Hosen, J. D.: Temperature, water travel time, and dissolved
397 organic matter structure river microbial communities in a large temperate watershed, Limnology
398 & Oceanography, 69, 1618–1635, https://doi.org/10.1002/lno.12591, 2024.

399 Becker, G., Dick, S., and Dippner, J.: Hydrography of the German Bight, Mar. Ecol. Prog. Ser., 91,
400 9–18, https://doi.org/10.3354/meps091009, 1992.

401 Bodelier, P. L. E. and Laanbroek, H. J.: Nitrogen as a regulatory factor of methane oxidation in
402 soils and sediments, FEMS Microbiology Ecology, 47, 265–277, https://doi.org/10.1016/S0168-
403 6496(03)00304-0, 2004.

404 Bodelier, P. L. E., Roslev, P., Henckel, T., and Frenzel, P.: Stimulation by ammonium-based
405 fertilizers of methane oxidation in soil around rice roots, Nature, 403, 421–424,
406 https://doi.org/10.1038/35000193, 2000.

407 Bussmann, I., Osudar, R., and Matousu, A.: Methane concentrations and methane oxidation rates
408 from Oct 2010 - Jun 2012 on a transect from Cuxhaven to Helgoland, North Sea, Germany,
409 https://doi.org/10.1594/PANGAEA.833798, 2014a.

410 Bussmann, I., Osudar, R., and Matousu, A.: Methane concentrations and methane oxidation rates
411 from Oct 2010 - March 2012 in the Elbe Estuary, from Hamburg to Cuxhaven, Germany,
412 https://doi.org/10.1594/PANGAEA.833923, 2014b.

413 Bussmann, I., Matousu, A., Osudar, R., and Mau, S.: Assessment of the radio^{3} H-CH_4 tracer
414 technique to measure aerobic methane oxidation in the water column, Limnology & Ocean
415 Methods, 13, 312–327, https://doi.org/10.1002/lom3.10027, 2015.

416 Bussmann, I., Hackbusch, S., Schaal, P., and Wichels, A.: Methane distribution and oxidation
417 around the Lena Delta in summer 2013, Biogeosciences, 14, 4985–5002,
418 https://doi.org/10.5194/bg-14-4985-2017, 2017.

419 Bussmann, I., Hackbusch, S., and Warnstedt, J.: Methane concentrations and methane oxidation
420 rates from Jan 2013 - Nov 2014 in the Elbe Estuary, from Hamburg to Helgoland, Germany,
421 https://doi.org/10.1594/PANGAEA.897351, 2019.

https://doi.org/10.5194/egusphere-2026-4822
Preprint. Discussion started: 24 August 2026

Dähnke, K., Sanders, T., Voynova, Y., and Wankel, S. D.: Nitrogen isotopes reveal a particulate-matter-driven biogeochemical reactor in a temperate estuary, Biogeosciences, 19, 5879–5891, https://doi.org/10.5194/bg-19-5879-2022, 2022.

Demeter, K., Savio, D., Kirschner, A. K. T., Reischer, G. H., Kolarevic, S., Parajka, J., Derx, J., Jakwerth, S., Wurzbacher, C., Blaschke, A. P., Mach, R. L., Blöschl, G., Farnleitner, A. H., and Eiler, A.: Hydrological regime of a continental river system predicts bacterial macroecological patterns, The ISME Journal, 19, wrag013, https://doi.org/10.1093/ismejo/wrag013, 2025.

Deng, Y., Liu, Y., Dumont, M., and Conrad, R.: Salinity Affects the Composition of the Aerobic Methanotroph Community in Alkaline Lake Sediments from the Tibetan Plateau, Microb Ecol, 73, 101–110, https://doi.org/10.1007/s00248-016-0879-5, 2017.

Egger, M., Riedinger, N., Mogollón, J. M., and Jørgensen, B. B.: Global diffusive fluxes of methane in marine sediments, Nature Geosci, 11, 421–425, https://doi.org/10.1038/s41561-018-0122-8, 2018.

Fofonova, V., Androsov, A., Sander, L., Kuznetsov, I., Amorim, F., Hass, H. C., and Wiltshire, K. H.: Non-linear aspects of the tidal dynamics in the Sylt-Rømø Bight, south-eastern North Sea, Ocean Sci., 15, 1761–1782, https://doi.org/10.5194/os-15-1761-2019, 2019.

Forster, P., Storelvmo, T., Armour, K., Collins, W., Dufresne, J. L., Frame, D., Lunt, D. J., Mauritsen, T., Palmer, M. D., Watanabe, M., Wild, M., and Zhang, H.: The Earth's Energy Budget, Climate Feedbacks, and Climate Sensitivity, in: Climate Change 2021: The Physical Science Basis, Cambridge University Press, Cambridge, United Kingdom and New York, NY, USA, 923–1054, https://doi.org/10.1017/9781009157896.009, 2021.

Gräwe, U., Flöser, G., Gerkema, T., Duran-Matute, M., Badewien, T. H., Schulz, E., and Burchard, H.: A numerical model for the entire Wadden Sea: Skill assessment and analysis of hydrodynamics, JGR Oceans, 121, 5231–5251, https://doi.org/10.1002/2016JC011655, 2016.

Grunwald, M., Dellwig, O., Beck, M., Dippner, J. W., Freund, J. A., Kohlmeier, C., Schnetger, B., and Brumsack, H.-J.: Methane in the southern North Sea: Sources, spatial distribution and budgets, Estuarine, Coastal and Shelf Science, 81, 445–456, https://doi.org/10.1016/j.ecss.2008.11.021, 2009.

Hackbusch, S., Wichels, A., and Bussmann, I.: Abundance, activity and diversity of methanotrophic bacteria in the Elbe Estuary and southern North Sea, Aquat. Microb. Ecol., 83, 35–48, https://doi.org/10.3354/ame01899, 2019.

Harpenslager, S. F., Randall, K., Zhu, Y., Jackson, M. C., Sanders, I., Gallo, B., Harris, D., Prentice, H., Bespalaya, Y. V., Aksenova, O. V., Milner, A., Cameron, T. C., McKew, B. A., O'Gorman, E. J., Yvon-Durocher, G., Friberg, N., Purdy, K. J., Woodward, G., Dumbrell, A. J., and Trimmer, M.: A fixed methane filter maximizes freshwater emissions under warming, Nat. Clim. Chang., 16, 704–711, https://doi.org/10.1038/s41558-026-02649-2, 2026.

Hermans, M., Stranne, C., Broman, E., Sokolov, A., Roth, F., Nascimento, F. J. A., Mörth, C.-M., Ten Hietbrink, S., Sun, X., Gustafsson, E., Gustafsson, B. G., Norkko, A., Jilbert, T., and Humborg,

https://doi.org/10.5194/egusphere-2026-4822
Preprint. Discussion started: 24 August 2026

C.: Ebullition dominates methane emissions in stratified coastal waters, Science of The Total Environment, 945, 174183, https://doi.org/10.1016/j.scitotenv.2024.174183, 2024.

Jacob, B. and Stanev, E. V.: Understanding the Impact of Bathymetric Changes in the German Bight on Coastal Hydrodynamics: One Step Toward Realistic Morphodynamic Modeling, Front. Mar. Sci., 8, 640214, https://doi.org/10.3389/fmars.2021.640214, 2021.

James, G., Witten, D., Hastie, T., and Tibshirani, R.: An Introduction to Statistical Learning: with Applications in R, Springer US, New York, NY, https://doi.org/10.1007/978-1-0716-1418-1, 2021.

Kappenberg, J. and Grabemann, I.: Variability of the Mixing Zones and Estuarine Turbidity Maxima in the Elbe and Weser Estuaries, Estuaries, 24, 699, https://doi.org/10.2307/1352878, 2001.

Kaupper, T., Mendes, L. W., Poehlein, A., Frohloff, D., Rohrbach, S., Horn, M. A., and Ho, A.: The methane-driven interaction network in terrestrial methane hotspots, Environmental Microbiome, 17, 15, https://doi.org/10.1186/s40793-022-00409-1, 2022.

Knief, C.: Diversity and Habitat Preferences of Cultivated and Uncultivated Aerobic Methanotrophic Bacteria Evaluated Based on pmoA as Molecular Marker, Front. Microbiol., 6, https://doi.org/10.3389/fmicb.2015.01346, 2015.

Lofton, D. D., Whalen, S. C., and Hershey, A. E.: Effect of temperature on methane dynamics and evaluation of methane oxidation kinetics in shallow Arctic Alaskan lakes, Hydrobiologia, 721, 209–222, https://doi.org/10.1007/s10750-013-1663-x, 2014.

Mao, S.-H., Zhang, H.-H., Zhuang, G.-C., Li, X.-J., Liu, Q., Zhou, Z., Wang, W.-L., Li, C.-Y., Lu, K.-Y., Liu, X.-T., Montgomery, A., Joye, S. B., Zhang, Y.-Z., and Yang, G.-P.: Aerobic oxidation of methane significantly reduces global diffusive methane emissions from shallow marine waters, Nat Commun, 13, 7309, https://doi.org/10.1038/s41467-022-35082-y, 2022.

Matousu, A., Osudar, R., Simek, K., and Bussmann, I.: Methane concentrations and methane oxidation rates from June 2012 - June 2013 in the Elbe Estuary, from Hamburg to Cuxhaven, Germany, https://doi.org/10.1594/PANGAEA.855825, 2015.

Matoušů, A., Osudar, R., Šimek, K., and Bussmann, I.: Methane distribution and methane oxidation in the water column of the Elbe estuary, Germany, Aquat Sci, 79, 443–458, https://doi.org/10.1007/s00027-016-0509-9, 2017.

Mayr, M. J., Zimmermann, M., Dey, J., Wehrli, B., and Bürgmann, H.: Lake mixing regime selects apparent methane oxidation kinetics of the methanotroph assemblage, Biogeosciences, 17, 4247–4259, https://doi.org/10.5194/bg-17-4247-2020, 2020.

Mohanty, S. R., Bodelier, P. L. E., and Conrad, R.: Effect of temperature on composition of the methanotrophic community in rice field and forest soil: Effect of temperature on soil methanotrophs, FEMS Microbiology Ecology, 62, 24–31, https://doi.org/10.1111/j.1574-6941.2007.00370.x, 2007.

https://doi.org/10.5194/egusphere-2026-4822
Preprint. Discussion started: 24 August 2026

Nijman, T. P. A., Amado, A. M., Bodelier, P. L. E., and Veraart, A. J.: Relief of Phosphate Limitation Stimulates Methane Oxidation, Front. Environ. Sci., 10, 804512, https://doi.org/10.3389/fenvs.2022.804512, 2022.

Nyerges, G., Han, S.-K., and Stein, L. Y.: Effects of Ammonium and Nitrite on Growth and Competitive Fitness of Cultivated Methanotrophic Bacteria, Appl Environ Microbiol, 76, 5648–5651, https://doi.org/10.1128/AEM.00747-10, 2010.

Osudar, R., Matoušů, A., Alawi, M., Wagner, D., and Bussmann, I.: Environmental factors affecting methane distribution and bacterial methane oxidation in the German Bight (North Sea), Estuarine, Coastal and Shelf Science, 160, 10–21, https://doi.org/10.1016/j.ecss.2015.03.028, 2015.

Osudar, R., Klings, K., Wagner, D., and Bussmann, I.: Effect of salinity on microbial methane oxidation in freshwater and marine environments, Aquat. Microb. Ecol., 80, 181–192, https://doi.org/10.3354/ame01845, 2017a.

Osudar, R., Klings, K., Wagner, D., and Bussmann, I.: Effect of salinity on microbial methane oxidation in freshwater and marine environments, Aquat. Microb. Ecol., 80, 181–192, https://doi.org/10.3354/ame01845, 2017b.

Oswald, K., Milucka, J., Brand, A., Hach, P., Littmann, S., Wehrli, B., Kuypers, M. M. M., and Schubert, C. J.: Aerobic gammaproteobacterial methanotrophs mitigate methane emissions from oxic and anoxic lake waters, Limnology & Oceanography, 61, https://doi.org/10.1002/lno.10312, 2016.

Plüß, Andreas: Das Nordseemodell der BAW zur Simulation der Tide in der Deutschen Bucht, Die Küste, 67, 84–127, 2003.

Russnak, V., Koll, R., Keuter, S., Sanders, T., and Dähnke, K.: The Elbe Estuary Microbiome Shifts With Salinity and Discharge and Depends on Fresh Organic Matter and Nutrient Availability, Environ Microbiol Rep, 18, e70349, https://doi.org/10.1111/1758-2229.70349, 2026.

Sanders, T., Schöl, A., and Dähnke, K.: Hot Spots of Nitrification in the Elbe Estuary and Their Impact on Nitrate Regeneration, Estuaries and Coasts, 41, 128–138, https://doi.org/10.1007/s12237-017-0264-8, 2018.

Scanlan, J., Guillonneau, R., Cunningham, M. R., Najmin, S., Mausz, M. A., Murphy, A., Murray, L. L., Zhang, L., Kumaresan, D., and Chen, Y.: The Proteobacterial Methanotroph Methylosinus trichosporium OB3b Remodels Membrane Lipids in Response to Phosphate Limitation, mBio, 13, e00247-22, https://doi.org/10.1128/mbio.00247-22, 2022.

Sherry, A., Osborne, K. A., Sidgwick, F. R., Gray, N. D., and Talbot, H. M.: A temperate river estuary is a sink for methanotrophs adapted to extremes of pH , temperature and salinity, Environ Microbiol Rep, 8, 122–131, https://doi.org/10.1111/1758-2229.12359, 2016.

Steinle, L., Graves, C. A., Treude, T., Ferré, B., Biastoch, A., Bussmann, I., Berndt, C., Krastel, S., James, R. H., Behrens, E., Böning, C. W., Greinert, J., Sapart, C.-J., Scheinert, M., Sommer, S.,

https://doi.org/10.5194/egusphere-2026-4822
Preprint. Discussion started: 24 August 2026

Lehmann, M. F., and Niemann, H.: Water column methanotrophy controlled by a rapid oceanographic switch, Nature Geosci, 8, 378–382, https://doi.org/10.1038/ngeo2420, 2015.

Steinle, L., Maltby, J., Treude, T., Kock, A., Bange, H. W., Engbersen, N., Zopfi, J., Lehmann, M. F., and Niemann, H.: Effects of low oxygen concentrations on aerobic methane oxidation in seasonally hypoxic coastal waters, Biogeosciences, 14, 1631–1645, https://doi.org/10.5194/bg-14-1631-2017, 2017.

Sundh, I., Bastviken, D., and Tranvik, L. J.: Abundance, Activity, and Community Structure of Pelagic Methane-Oxidizing Bacteria in Temperate Lakes, Appl Environ Microbiol, 71, 6746–6752, https://doi.org/10.1128/AEM.71.11.6746-6752.2005, 2005.

Tobias-Hünefeldt, S. P., Woodhouse, J. N., Ruscheweyh, H.-J., Sunagawa, S., Russnak, V., Streit, W. R., and Grossart, H.-P.: Osmotolerance is a driver of microbial carbon processes in the Elbe estuary, mSystems, 11, e01790-25, https://doi.org/10.1128/msystems.01790-25, 2026.

Tveit, A. T., Söllinger, A., Rainer, E. M., Didriksen, A., Hestnes, A. G., Motleleng, L., Hellinger, H.-J., Rattei, T., and Svenning, M. M.: Thermal acclimation of methanotrophs from the genus Methylobacter, The ISME Journal, 17, 502–513, https://doi.org/10.1038/s41396-023-01363-7, 2023.

Weber, T., Wiseman, N. A., and Kock, A.: Global ocean methane emissions dominated by shallow coastal waters, Nat Commun, 10, 4584, https://doi.org/10.1038/s41467-019-12541-7, 2019.

Wilkins, D., Lauro, F. M., Williams, T. J., Demaere, M. Z., Brown, M. V., Hoffman, J. M., Andrews-Pfannkoch, C., Mcquaid, J. B., Riddle, M. J., Rintoul, S. R., and Cavicchioli, R.: Biogeographic partitioning of S outhern O cean microorganisms revealed by metagenomics, Environmental Microbiology, 15, 1318–1333, https://doi.org/10.1111/1462-2920.12035, 2013.